How to measure the area of real contact of skin on glass

Huloux, Nicolas; Willemet, Laurence; Wiertlewski, Michael

DOI
10.1109/TOH.2021.3073747

Publication date
2021

Document Version
Accepted author manuscript

Published in
IEEE Transactions on Haptics

This article has been accepted for publication in a future issue of this journal, but has not been fully edited. Content may change prior to final publication. Citation information: DOI 10.1109/TOH.2021.3073747, IEEE Transactions on Haptics

How to measure the area of real contact of skin on glass

Nicolas Huloux, Laurence Willemet, and Michaël Wiertlewski *Member, IEEE*

***Abstract*—The contact between the fingertip and an object is formed by a collection of micro-scale junctions, which collectively constitute the real contact area. This real area of contact is only a fraction of the apparent area of contact and is directly linked to the frictional strength of the contact (i.e., the lateral force at which the finger starts sliding). As a consequence, a measure of this area of real contact can help probe into the mechanism behind the friction of skin on glass. In this article, we present two methods to measure the variations of contact area; one that improves upon a tried-and-true fingertip imaging technique to provide ground truth, and the other that relies on the absorption and reflection of acoustic energy. To achieve precise measurements, the ultrasonic method exploits a recently developed model of the interaction that incorporates the non-linearity of squeeze film levitation. The two methods are in good agreement ($\rho = 0.94$) over a large range of normal forces and vibration amplitudes. Since the real area of contact fundamentally underlies fingertip friction, the methods described in the article have importance for studying human grasping, understanding friction perception, and controlling surface-haptic devices.**

***Index Terms*—Biomechanics, Tactile devices, Sensors, Acoustic waves, Contact Imaging**

I. Introduction

Friction underpins most tactile interactions. It is necessary for grasping objects [1] and its variation during tactile exploration helps distinguish material properties [2]–[4]. The exquisite sensitivity to change of friction has not escaped the notice of engineers. Consequently, they have developed surface-haptic interfaces which rely on the real-time modulation of friction to create convincing sensations of texture [5]–[7], shape [8], and even stickiness [9].

At a macroscopic scale, the frictional strength of a contact is typically found from the lateral force at which relative motion occurs [10]. But even when no tangential force is exerted, this frictional strength is present, since the intimate contact of skin on the surface holds a potential for adhesion. There is evidence that the somatosensory system recognizes the frictional strength at the early stages of contact [11]. Therefore, being able to measure the frictional strength without sliding can lead to a better understanding of human sensory mechanisms as well as offer a new outlook for controlling surface haptics.

At the microscopic scale, the contact between the skin and an atomically-flat surface is made by a collection of individual junctions of a micrometer-scale area. The sum of the areas of all junctions constitutes the real area of contact [12]. An increase in normal force will create more junctions, each of which will have a larger area. Each of these junctions can carry a certain amount of shear stress τ_0 before local sliding can occur, and therefore the friction force can be found to be linearly related to the real area of contact such that $f_t = \tau_0 A^R$.

This linear dependence is observed for a large set of materials including rubbery and biological materials [13]–[15]. Thus, a powerful method to estimate the frictional resistance of a contact, even before the fingertip starts sliding, is to measure an approximation of the real contact area directly.

N. Huloux and L. Willemet are with Aix-Marseille Univ., CNRS, ISM, Marseille France

M. Wiertlewski is with TU Delft, Delft, The Netherlands.

This research was supported by the Agence Nationale de la Recherche project IOTA 16-CE33-0002 and project PHASE 16-CE10-0003

An accurate measurement of the real area of contact can be found by optical means in the case of biological materials such as glabrous skin. As a testament to their efficacy, the measurements reported by these methods correlate with friction force confirming the adhesive theory of friction even in the case of soft materials [15], [16]. One of the major drawbacks of optical methods, however, is their reliance on bulky optical components and computationally-expensive image processing.

As an alternative to optical means, absorption and reflection of acoustic waves can also provide a measure of the real area of contact in rigid and soft materials [17]–[20]. To the best of our knowledge, these methods have not been applied to the contact with a fingertip. We recently showed that ultrasonic waves created to modulate friction on a surface haptics device, reduce the size and the number of junctions and by extension the real area of contact [15], [21]. The vibration of the plate creates a levitation pressure, thereby reducing the number of asperities in contact. During this process, a portion of the acoustic energy is transferred to the fingertip [21], [22]. Upon a change in normal force or actuation force, we observe that both the contact and the impedance are affected, see Fig. 1. Here, we hypothesize that the ultrasonic impedance can be used to measure an approximation of the area of real contact, without fingertip slippage and provide a surrogate measure of the frictional strength of the contact.

To test this hypothesis, we developed a dedicated apparatus to simultaneously measure the area of real contact and the ultrasonic impedance. The two variables correlate strongly for every subject (Pearson correlation coefficient $\rho = 0.94$), confirming the hypothesis. We discuss the implications of such measurement for precisely controlling friction on surface haptic interfaces, even before the finger starts sliding.

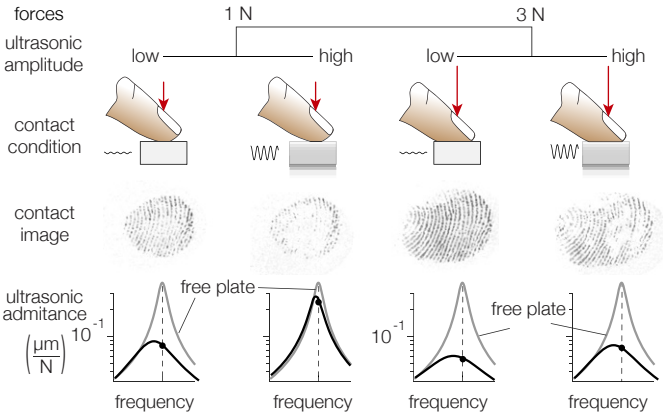

Fig. 1. Illustration of the simultaneous variation of real contact area optically estimated and of the plate impedance for two normal forces and two ultrasonic levitation magnitudes. Low normal forces produce small values of the real and the apparent contact area. Only the real contact area is affected by ultrasonic levitation. The admittance plots illustrate the attenuation of the plate vibration caused by the presence of a fingertip. High actuation forces induce a levitation of the skin, which reduces the amount of attenuation provided by the skin.

This article has been accepted for publication in a future issue of this journal, but has not been fully edited. Content may change prior to final publication. Citation information: DOI 10.1109/TOH.2021.3073747, IEEE Transactions on Haptics

II. How to measure real area of contact from images

A. Self-similar model and physical real area

The height profile of the skin approximately follows a self-affine fractal [23]. Similar roughness patterns can be observed at different magnifications. As a consequence, it is relevant to understand the physics behind the contact area measurement of the rough skin on an atomically flat glass surface using multi-scale theory [12].

The theory notes that when pressing a randomly rough surface onto another, the contact exists only between the highest asperities, forming distinct junctions between the two surfaces. However, if one magnifies the view to only one junction, it appears that it refines in a multitude of smaller junctions. Magnifying even more would reveal another set of even smaller junctions, and so on. This process can theoretically continue to infinity, at which point the real area of contact disappears. A similar paradox is famously found when measuring the length of the coast of Britain with an increasingly smaller measurement quantum [24].

However, the decrease in the real area of contact for increasing magnification stops at a certain cut-off. One of the reasons, relevant in the case of the skin, is that for a given normal force, the interfacial stress increases with increasing magnification until it reaches the yield stress of the material. At that point, the asperities deform plastically, and the local contact is total at that scale. Estimates place the ultimate size of a junction for dry skin in the 1 to 10 μm range [16], [25].

Optical methods have a resolution limited by the half-wavelength of light ($\approx$ 300 nm in our case). They are therefore ideal to image in sufficient detail the physical real area of contact made by the plasticized junction. In this work, images provide ground truth for alternative methods such as the ultrasonic one.

B. Separating asperities from background with frustrated reflection

Two optical methods separate junctions from the background by using the principle of frustrated reflection. When an incident light ray is reflected at the interface between glass and air, either totally [15], [26]–[28] or partially [16], [29], [30], an electromagnetic wave field is present on the opposite side of the interface. This transmitted wave field can either be evanescent in the case of a total internal reflection (i.e., if the incident beam is at a shallow angle with the surface) or a plane wave in the case of an orthogonal reflection (i.e., when the incident beam is exactly perpendicular to the surface). When the asperities of the skin couple with the transmitted wave field, the reflected light is absorbed and scattered. This scattering creates darker regions in the reflected image and provides a highly contrasted image of the individual asperities in intimate contact.

Here, we use the coaxial method, leveraging an illumination orthogonal to the surface. The illumination setup is illustrated Fig. 2a, and the influence of the skin on the reflection is illustrated Fig. 2b. The resulting images can be seen in Fig. 2c, with and without the presence of a fingertip.

C. Imager quantization

The reflected image highlighting the region where no asperities are in contact and darkening the region of intimate contact is sampled with a camera. During this process, the number of photons collected on each pixel is inversely correlated to the number of asperities present in the region imaged by the pixel. If the exposure of the camera is fixed, the brightness field corresponds to an inverse image of the density of junctions resolved at a length scale comparable to the half-wavelength of light. Darker areas represent a higher density of asperities in intimate contact.

To capture this reflected image, the camera sensor discretizes the number of photons collected during the exposure. The darker

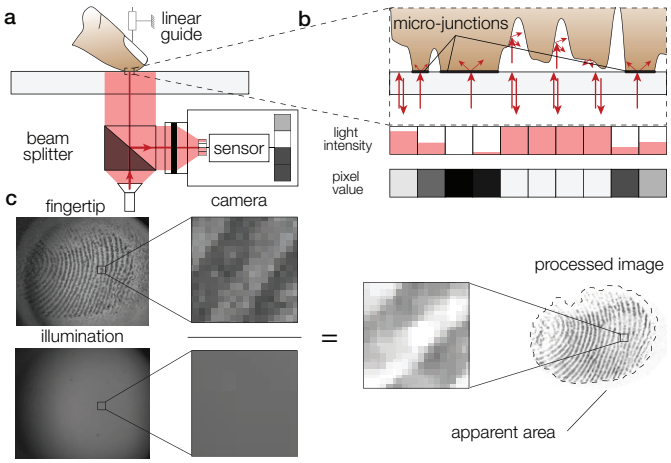

Fig. 2. **a**. Imaging apparatus used to measure an estimate of the real contact area. A light source shines perpendicularly to the glass plate. At the boundary between glass and air, four percent of the light reflects in parallel to the incident beam. The presence of the skin scatters the incident light rays, creating a darker area on the reflected image, which is then captured by the camera via a beam splitter. **b**. Each pixel collects a number of photons inversely proportional to the number of microscopic asperities in contact with the plate. This quantity is then converted into grayscale by the camera. **c**. To recover an approximation of the real contact area, we divided pixel-wise the fingertip image by the illumination image which was corrected for the non-uniform lighting. The brightness of the inverse of the resulting image is a direct measure of the optical area of contact.

areas receive fewer photons and lead to a lower value of the pixels. Conversely, the areas that do not face any finger asperities receive the maximum number of photons per unit area. Therefore, we can set the exposure such that this maximum number of photons induces a value of the pixel that reaches the top of the dynamic range.

D. Reflectance as a measure of the contact area

From the high-contrast image, it is possible to recover a value that is proportional to the area of real contact at half-wavelength of light lengthscale. The principle is described in figure 2c and d. First, consider the image without a fingertip, which might have a non-uniform illumination. The resulting background image I_0 corresponds to the dynamic range of each pixel. To normalize the illumination on every subsequent image of the contact I_f, we use a pixel-to-pixel division of the image by the background image. Once this is done, the normalized image is inverted to find the estimate of the light absorbed by the contact I_a such that:

$$I_a = 1 - I_f / I_0 \tag{1}$$

The contact area is therefore found by summing the brightness of every pixel of the absorption image I_a.

The *absorbed-light method* provides a granular measurement of the fractal real contact area, with a theoretical resolution at the wavelength of the incident light, which is in the order of 300 nm. The resolution is orders of magnitude better than a simple thresholding and pixel-counting procedure, used in [16], [31] for instance. The reason is that thresholding places the effective resolution at the size of a pixel, which is in the order of tens of micrometers. Finally, the optical estimation of the real area of contact A^O is calibrated using a measurement of the apparent area of contact, A^A, expressed in mm, knowing that the real and apparent area are identical in the hypothetical case that the contact is total.

This article has been accepted for publication in a future issue of this journal, but has not been fully edited. Content may change prior to final publication. Citation information: DOI 10.1109/TOH.2021.3073747, IEEE Transactions on Haptics

III. How to measure real area of contact from mechanical impedance

The amount of skin in contact has a dramatic effect on the absorption and scattering of ultrasonic waves. A plate that vibrates at ultrasonic frequencies with amplitude up to several micrometers when no load is present, can see its amplitude decay by 90% of its value when a finger touches it [32]. Given that the piezoelectric actuator provides the same harmonic force with or without the presence of a finger, a decrease in vibration amplitude signifies that the impedance of the plate-finger system is higher than the one of the plate itself. We previously showed that the variation of the system impedance can predict the friction force of a sliding finger [21]. Since the friction force is directly dependent on the real area of contact, could it be that the variations of impedance reflect the amount of contact between the skin and the plate?

One of the key insights is to consider the variation of the impedance of the plate-finger system to be caused by the impedance of the tissues, denoted Z_t, and a locally linear impedance coupling the dynamics of the plate to the dynamics of the skin, denoted Z_c. Despite the presence of a highly non-linear levitation process, the system impedance has a surprisingly low harmonic content and is invariant with time in the normal operation of the device [21]. Based on the experimental evidence, we can safely assume that the impedance Z_c is a locally linear-time-invariant system, at least for a given amplitude of vibration, a given normal force, and a given frequency.

However, the value of this coupling impedance is not fixed and varies with the normal force and the amplitude of the ultrasonic vibration. This dependence stems from the squeeze-film levitation that is created at the interface, which levitates the skin thereby reducing the acoustic transmissivity of the interface.

A. Finding the contact impedance

The ultrasonic plate is excited by piezoelectric actuators glued to its surface. Close to the resonant frequency, the dynamics resemble a linear mass-spring-damper system excited with a harmonic force f_a, which is directly proportional to the voltage applied to the electrodes of piezoelectric elements. The proportionality factor is found by fitting a second-order model to the measured frequency response of the unloaded plate, using the mass of the glass plate to find the proper scale, see [33] for complete derivation. This force causes the plate and everything in contact with it, to oscillate into a harmonic motion of instantaneous velocity v_p. The impedance is defined by the complex-valued ratio of the force over the velocity. In the case of the finger contacting the plate, however, the dynamic system is slightly more complex and involves multiple lumped impedances: one for the plate Z_p, one for the skin tissues Z_t and one for the interface Z_c. A free-body diagram of the model can be found in figure 3a.

Knowing the plate impedance, by assuming a second-order dynamics around the resonant frequency, and the impedance of the tissues, we can measure the contact impedance by noting that:

$$Z_m = \frac{v_p}{f_a} = Z_p + \frac{Z_t\, Z_c}{Z_t + Z_c} \tag{2}$$

The measured impedance Z_m is the sum of the plate impedance and the parallel association of the contact impedance and the tissues impedance. We assume that the plate impedance is constant during one interaction. The impedance of the tissues Z_t is estimated offline for every subject from the trials where the actuation force is 5 mN and the contribution of ultrasonic levitation is assumed negligible.

B. Experimental determination

Figure 3b illustrates the method to recover the contact impedance. The force applied by the piezoelectric elements f_a and the velocity v_p

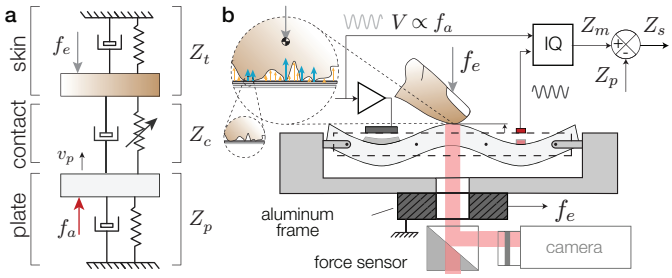

Fig. 3. **a**. Two-degree-of-freedom model of the interaction between a fingertip and an ultrasonic vibrating plate, from [21]. **b**. Experimental setup used for inducing squeeze film levitation and measuring impedance in real-time. Piezoelectric actuators force the plate to bend with a harmonic force f_a. The motion of the plate is found using a calibrated piezoelectric sensor. The vibrating plate is attached to an aluminum frame by its nodal-lines, connected to a six-axis force sensor. The harmonic force and displacement are IQ demodulated to find the complex-valued impedance Z_m. Subtracting the unloaded plate impedance Z_p gives the impedance variation Z_s.

are demodulated using IQ demodulation. This demodulation converts the time domain harmonic signal into in-phase and quadrature signals that correspond to the Fourier coefficient of the signal at the frequency of excitation. This demodulation allows for tracking the real-time variation of the relative phase and magnitude between the two signals, encapsulated in the impedance Z_m. At this stage, the unloaded plate impedance Z_p is removed from the measured impedance Z_m, focusing only on the variation caused by the fingertip $Z_s = \frac{Z_t\, Z_c}{Z_t + Z_c}$.

C. Contact impedance and real area of contact

The impedance of the tissues Z_t can be safely assumed to be constant for a given participant and a given lapse of time. The only contributor to the variation of the system impedance is therefore the impedance that models the behavior of the interface Z_c. This impedance represents the acoustic transmissivity of the plate vibrations to the skin tissues. Since the interface is composed of a collection of asperities in intimate contact, this transmissivity is favored by a larger number of asperities, thus a larger contact area.

The contact impedance is influenced by both the amount of normal force applied by the finger f_e and the levitation force applied by the actuator on the plate f_a. An increase in the normal force brings the two surfaces closer together and enlarges the number of asperities in contact. Conversely, higher levitation forces, created by squeeze-film, push the asperities away from the plate and reduce the transmissivity of the interface.

In [21], we used multi-scale contact theory to derive a numerical expression that links the interfacial gap and the impedance of the interface. Since the interfacial gap evolves logarithmically with the real area of contact at a given scale, a causal relationship exists between this real area of contact and the impedance variations. The following shows the experimental validation of this hypothesis.

IV. Material and methods

A. Apparatus for imaging contact during friction modulation

The ultrasonic friction modulation device used in this study is made of a borosilicate glass plate of dimension $67 \times 50 \times 5$ mm^3. The 3×0 mode of the plate is excited at 29194 Hz by piezoelectric actuators. The actuators are fed by a high voltage harmonic signal amplified $\times 20$ (WMA-100, Falco Systems, Katwijk, Netherlands). The plate vibrations are measured by a smaller piezoelectric element whose output has been calibrated with an interferometer (DS 3010, Attocube, Munich, Germany). This plate is secured on an aluminum frame by four nylon-tip screws pressing on the nodal lines. The

This article has been accepted for publication in a future issue of this journal, but has not been fully edited. Content may change prior to final publication. Citation information: DOI 10.1109/TOH.2021.3073747, IEEE Transactions on Haptics

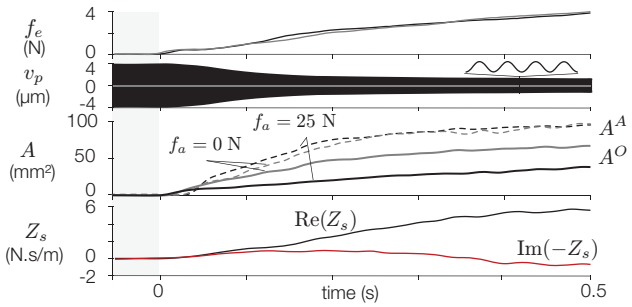

Fig. 4. Typical trial showing the normal force, the plate vibration, the optical estimate of the real A^O and apparent A^A areas of contact, and system mechanical impedance. A high actuation force $f_a = 25$ N is shown in black and $f_a = 0$ N is shown in grey.

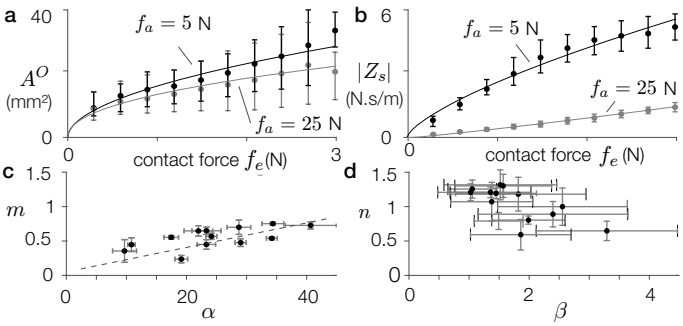

Fig. 5. Optical estimations of the real area of contact (**a**) and mechanical system impedance modulus (**b**) of a typical subject function of the contact force for two actuation forces $f_a = 5$ N (black) and $f_a = 25$ N (grey). Individual dots represent the mean of six interactions under one actuation force. Error bars stand for the standard deviation over one condition. The power law is represented by solid lines. The fitting parameters α and m (**c**) such as β and p (**d**) of each subject, where black dots represent the mean over every actuation force and error bars the distribution. The dashed line represents the linear regression of the data set (Pearson correlation coefficient $\rho = 0.63$).

interaction forces are recorded by a 6-axis force sensor (Nano 43, ATI, Apex, USA). The coaxial illumination is provided by a red-light source (M660L4, Thorlabs, Newton, USA), shone through a beam-splitter toward the plate. The red color is chosen for its high absorption by the skin, increasing the contrast. The incident beam hits the plate orthogonally. The beam-splitter reflects the returning beam to a high-speed camera (VEO E310, Phantom, Wayne, USA), which captures images at 300 Hz. Fig. 3b shows an illustration of the complete apparatus.

B. Experimental Protocol

Fourteen right-handed volunteers, three females and eleven males from 19 to 55 years old participated in the study. The result of one subject was discarded due to technical issues. The study was conducted with the approval of the Aix-Marseille Université ethics committee and the participants gave their informed consent prior to the experiment. They were asked to press on the vibrating plate with an approach angle of 30° to the plate surface. The nail of the index finger was firmly attached with a clip to a vertical linear guide avoiding any lateral motion of the finger. Seven actuation forces from 0 to 30 N have been presented to subjects six times each, resulting in a total of 42 fingertip interactions of about a second per subject. The actuation forces were held constant during each individual trial and induced a range of vibration from 0 to 3 µm of amplitude to the unloaded plate. Force and image recordings were synchronized with a trigger signal sent to the camera when the finger started touching the surface. Time series of a typical trial are shown in Fig. 4.

V. Results

A. Optical area of contact and impedance

According to multi-scale contact theory, the real area of contact linearly correlates with the applied pressure [12]. While this assumption holds for flat or infinite surfaces, the fingertip has a spherical shape, therefore, an increase in normal force also increases the apparent contact area, following Hertzian contact theory. The increase of apparent area is working alongside the increase in asperities density resulting in a non-linear relationship, see Fig. 5a. To capture this phenomenon, we fitted the optical measurement of the real contact area to a two-parameter power law:

$$A^O = \alpha\, f_e^m \tag{3}$$

where α is the proportional coefficient and m is the exponent. The procedure used Levenberg–Marquardt curve-fitting algorithm and the resulting parameters for every subject are shown in Fig. 5a. The goodness of fit of the power law on the experimental data ranges from $R^2 = 0.87 \pm 0.15$. The exponent varied between 0.19 and 0.91, while the coefficient of proportionality varied from 11.2 to 51.3 $\mathrm{mm}^2.\mathrm{N}^{-1}$. Interestingly, the mean of the load index and of the proportionality coefficient of each subject are correlated with a Pearson correlation coefficient of $\rho = 0.63$. We do not exclude that this correlation could be due to an artifact. The intra-subject variability of the exponent is within the size of its average value with a standard deviation of $\sigma(m) = 0.17 \pm 0.04$. The proportionality coefficient and the exponent negatively correlate with the actuation force f_a (Pearson coefficient $\rho = -0.89$ for α and $\rho = -0.79$ for m).

As expected, the impedance also showed a correlation with the applied force f_e and with the levitation force f_a. We applied a similar curve fitting procedure to the modulus of the impedance variation $|Z_s|$ expressed as a function of the contact force f_e with:

$$|Z_s| = \beta\, f_e^n \tag{4}$$

with β the proportionality coefficient and n the exponent. The optimization leads to a goodness of fit of $R^2 = 0.9 \pm 0.1$ over all trials. Typical data are shown in Fig. 5b and results on all trials and all participants are shown in Fig. 5d. The coefficient of proportionality β ranges from 1.01 and 7.59 $\mathrm{s.m}$ and the exponent from 0.34 to 1.56. The intra-subject variability of the exponent is also within the size of its average value with a standard deviation of $\sigma(n) = 0.26 \pm 0.14$. The proportionality coefficient negatively correlates with the actuation force f_a while the exponent positively does (Pearson coefficient $\rho = -0.63$ for β and $\rho = 0.87$ for n).

B. Area of contact as a function of impedance

The relation between the optical estimation of the contact area A^O and the impedance is shown Fig. 6a for a typical subject at $f_a = 5$ and $f_a = 25$ N actuation force. Following the same idea as earlier, we performed a nonlinear regression on the scatter plot with a power law function: $A^O = \gamma\, |Z_s|^p$. The regression leads to a goodness of fit of $R^2 = 0.8 \pm 0.25$. The values of the proportionality coefficient γ and the exponent p are reported in Fig. 6b and c for all subjects at each actuation force. The proportionality coefficient γ increases with actuation force whereas the exponent p decreases. Consequently, the relation between the optical contact area and the system impedance modulus deviates from linearity as the actuation force increases.

As expected, we find that $\gamma \approx \alpha/(\beta)^{\frac{m}{n}}$ and $p \approx m/n$ with less than 10% of error over all subjects and actuation forces. This

This article has been accepted for publication in a future issue of this journal, but has not been fully edited. Content may change prior to final publication. Citation information: DOI 10.1109/TOH.2021.3073747, IEEE Transactions on Haptics

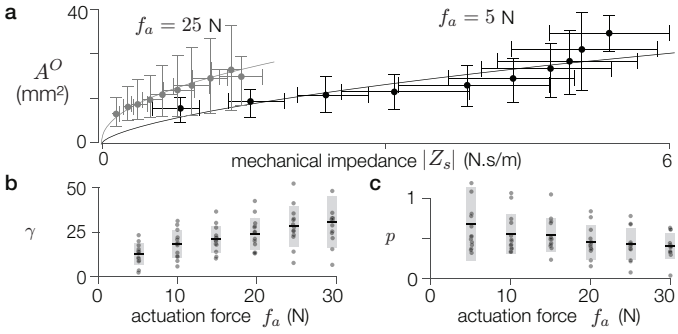

Fig. 6. **a**. Scatter plot of the optical contact area and the impedance for one typical subject at $f_a = 5$ N (grey) and $f_a = 25$ N (black). Individual dots represent the mean of the six interactions of each actuation force and error bars the standard deviation. The scatter plots have been fitted with a power law for every actuation force, represented in solid lines. The proportionality coefficient, γ (**b**), and exponent, p (**c**), of the regression function, are displayed along with the actuation force (Pearson coefficient $\rho = 0.98$ and $\rho = -0.41$ respectively), where black dots represent individual datum of each subject, black lines are the mean and grey boxes the standard deviation.

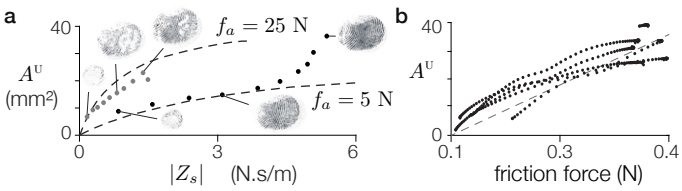

Fig. 7. **a**. Estimations of the real area of contact from the optical measurements together with estimations from impedance and the multi-scale contact model. The dashed lines represent a simulation of this model with the parameters $\sigma_t = 18$ µm and $E = 40$ MPa for two activation forces. Optical data points are shown as dots. **b**. Estimated area of contact from the acoustic impedance as a function of the measured friction force measurements. Data represent five sliding interactions on a 6 Hz modulated ultrasonic vibrating plate taken from [21]. Dots are individual datum and the dashed line shows the linear approximation.

empirical power law model can predict the optical area of contact from the impedance with a mean error of $3.3\ \mathrm{mm}^2$ over $38.2\ \mathrm{mm}^2$ of mean area of contact for 3 N of contact force.

C. Agreement between methods

The mechanical impedance correlates significantly with the optical measurement of the real contact area, but only for a given amplitude of vibration including quasi-static conditions where levitation has a negligible effect. The actuation force modifies the relationship, which hints at a more complex behavior of the impedance. To gain insight, we simulated the behavior using the dynamic model presented in Fig. 3a, which contains a non-linear element transferring energy from the plate to the fingertip. As fully described in [21], this Kelvin-Voigt element is non-linearly affected by the number of asperities in contact and the force of the acoustic levitation. This model uses Reynolds' equation and multi-scale contact model to estimate the contact impedance Z_c as a function of the average interfacial separation, the contact force, and the actuation force. The model takes the impedance as input and outputs an estimate of the area of contact A^{U}, as shown in Fig. 7a. The predictions of the model also follow a power law function. The proportionality coefficient and exponent are close to the optical data, with an error of $8 \pm 9\%$ for the proportionality coefficient and $17 \pm 9\%$ for the exponent, over all subjects and all actuation forces.

The method applied on the dataset of [21], shows that the friction force and the ultrasonic estimation of the area of contact agreed (Pearson correlation coefficient $\rho = 0.98$, $p = 10^-21$), see Fig.7.

VI. Discussion

A. Friction-modulation does not reduce contact area homogeneously

Large ultrasonic oscillations lift the skin over the plate, thereby reducing the quantity of micro-junctions. The images offer a way to observe the spatially-resolved evolution of the contact. Interestingly, within the area of contact, certain regions completely disappear, while others remain attached. Since the contact is assumed to follow a random profile of asperities height [12], it is clear that the brightness of each pixel corresponds to the density of asperities in intimate contact. When pixels have values close to the background illumination, it indicates that the contact has completely vanished under the effect of the ultrasonic levitation. Since the change is not uniform throughout the image, there is also evidence that the levitation is not homogeneous. Similar disappearance of micro-contacts phenomenon exists during rough contact sliding [16], although in the case of that study image thresholding was used.

B. The real area of contact follows a power law with contact force

The evolution of the apparent contact area under an increasing normal force has been widely studied in the literature. Its behavior is well approximated by a Hertzian contact model, leading to a power law, of exponent 2/3, that predicts the apparent contact area from the normal force. Some optical measurements of the apparent area found in the literature report also an exponent close to 2/3 [34], consistent with the theory. Other fingertip studies found various exponents for the area within the apparent area of contact (*i.e.*, at a smaller scale), one that is $\approx 2/3$ [35], another is $\approx 1/2$ [31], and ≈ 0.4 [36]. These differences could be attributed to variations in measurement method but also to fingertips mechanical parameters. In the present study, the frictional behavior of the fingertip of 13 participants has been investigated. Our measurement shows that the exponent varies from $\approx 1/3$ to $\approx 2/3$, covering the range found in the literature. Using our model, we estimate that the mechanical properties of skin are $E = 68 \pm 52$ MPa for the Young modulus, and $\sigma_t = 19 \pm 9.2$ µm for the average roughness height distribution.

As a testimony to reinforce this intuition, in our study, the linear coefficient and the exponent parameters that fit the data are correlated (Pearson correlation coefficient $\rho = 0.65$). Besides, in Hertz theory, the linear coefficient of the power law is related to the stiffness and the shape of the contact, so the exponent might be also related to these mechanical parameters.

C. Implication for surface haptics

Surface haptic interfaces produce tactile sensations by modulating friction of the user's bare fingertip. One major issue they face is the high variability of the frictional behavior of fingertips [37] that renders the stimulation imprecise. One way to overcome this variability is to measure and control friction via a control loop [7], [38], [39]. The tribometer used to measure the friction in these studies limits the control only on sliding moments of the fingertip. Hence, the measure of static friction is only possible at the very moment of sliding, forcing the rendering of stiction to rely on models [9]. The method presented here does not require lateral motion to assess the frictional resistance of the fingertip on the surface. Also, the estimation has low computational effort, which allows for high-speed closed-loop control. However, only one value of the impedance can be measured, which prohibits multi-touch interaction.

Expanding this method to glass/polymer contact could be used to estimate friction strength on robotic grippers at initial contact.

VII. Conclusion

The real area of contact offers a unique picture of the frictional interaction between the skin and a surface. In this work, we reviewed and improved the optical methods to reliably measure this quantity. In addition, we introduce a new method that advantageously exploits the presence of ultrasonic waves in surface haptic devices to extract a measurement of the real area of contact. Both methods agreed in the quasi-static cases of a pure normal press and of a steady sliding.

This new method enables the measurement of an estimate of the real contact area, in every situation where optical methods would be too cumbersome. Moreover, the method only requires inexpensive piezoelectric sensors, already present in most surface-haptic devices. Finally, because of low computational effort, this method is suited for a closed-loop control on the real area of contact, necessary for high-fidelity surface haptics.

References

[1] G. Cadoret and A. M. Smith, "Friction, not texture, dictates grip forces used during object manipulation," *Journal of neurophysiology*, vol. 75, no. 5, pp. 1963–1969, 1996.

[2] A. M. Smith, C. E. Chapman, M. Deslandes, J.-S. Langlais, and M.-P. Thibodeau, "Role of friction and tangential force variation in the subjective scaling of tactile roughness," *Experimental brain research*, vol. 144, no. 2, pp. 211–223, 2002.

[3] M. Wiertlewski, J. Lozada, and V. Hayward, "The spatial spectrum of tangential skin displacement can encode tactual texture," *IEEE Transactions on Robotics*, vol. 27, no. 3, pp. 461–472, 2011.

[4] D. Gueorguiev, S. Bochereau, A. Mouraux, V. Hayward, and J.-L. Thonnard, "Touch uses frictional cues to discriminate flat materials," *Scientific reports*, vol. 6, p. 25553, 2016.

[5] M. Biet, G. Casiez, F. Giraud, and B. Lemaire-Semail, "Discrimination of virtual square gratings by dynamic touch on friction based tactile displays," in *2008 symposium on haptic interfaces for virtual environment and teleoperator systems*. IEEE, 2008, pp. 41–48.

[6] C. Bernard, J. Monnoyer, and M. Wiertlewski, "Harmonious textures: The perceptual dimensions of synthetic sinusoidal gratings," in *International Conference on Human Haptic Sensing and Touch Enabled Computer Applications*. Springer, 2018, pp. 685–695.

[7] R. V. Grigorii and J. E. Colgate, "Closed loop application of electroadhesion for increased precision in texture rendering," *IEEE Transactions on Haptics*, vol. 13, no. 1, 2020.

[8] Y. Vardar, B. Güçlü, and C. Basdogan, "Effect of waveform on tactile perception by electrovibration displayed on touch screens," *IEEE transactions on haptics*, vol. 10, no. 4, pp. 488–499, 2017.

[9] R. V. Grigorii, M. A. Peshkin, and J. E. Colgate, "Stiction rendering in touch," in *2019 IEEE World Haptics Conference (WHC)*. IEEE, 2019.

[10] A. Barrea, D. C. Bulens, P. Lefèvre, and J.-L. Thonnard, "Simple and reliable method to estimate the fingertip static coefficient of friction in precision grip," *IEEE transactions on haptics*, vol. 9, no. 4, 2016.

[11] R. S. Johansson and G. Westling, "Roles of glabrous skin receptors and sensorimotor memory in automatic control of precision grip when lifting rougher or more slippery objects," *Experimental brain research*, vol. 56, no. 3, pp. 550–564, 1984.

[12] B. Persson, O. Albohr, C. Creton, and V. Peveri, "Contact area between a viscoelastic solid and a hard, randomly rough, substrate," *The Journal of chemical physics*, vol. 120, no. 18, pp. 8779–8793, 2004.

[13] F. P. Bowden and D. Tabor, "The area of contact between stationary and moving surfaces," *Proceedings of the Royal Society of London. Series A. Mathematical and Physical Sciences*, vol. 169, no. 938, 1939.

[14] M. Barquins and A. Roberts, "Rubber friction variation with rate and temperature: some new observations," *Journal of Physics D: Applied Physics*, vol. 19, no. 4, p. 547, 1986.

[15] M. Wiertlewski, R. F. Friesen, and J. E. Colgate, "Partial squeeze film levitation modulates fingertip friction," *Proceedings of the national academy of sciences*, vol. 113, no. 33, pp. 9210–9215, 2016.

[16] R. Sahli, G. Pallares, C. Ducottet, I. B. Ali, S. Al Akhrass, M. Guibert, and J. Scheibert, "Evolution of real contact area under shear and the value of static friction of soft materials," *Proceedings of the National Academy of Sciences*, vol. 115, no. 3, pp. 471–476, 2018.

[17] K. Kendall and D. Tabor, "An utrasonic study of the area of contact between stationary and sliding surfaces," *Proceedings of the Royal Society of London. A. Mathematical and Physical Sciences*, vol. 323, no. 1554, pp. 321–340, 1971.

[18] J. Krolikowski and J. Szczepek, "Prediction of contact parameters using ultrasonic method," *Wear*, vol. 148, no. 1, pp. 181–195, 1991.

[19] M. Pau, F. Aymerich, and F. Ginesu, "Ultrasonic measurements of nominal contact area and contact pressure in a wheel-rail system," *Proceedings of the Institution of Mechanical Engineers, Part F: Journal of Rail and Rapid Transit*, vol. 214, no. 4, pp. 231–243, 2000.

[20] F. Aymerich and M. Pau, "Assessment of nominal contact area parameters by means of ultrasonic waves," *J. Trib.*, vol. 126, no. 4, 2004.

[21] N. Huloux, C. Bernard, and M. Wiertlewski, "Estimation of the modulation of friction from the mechanical impedance variations," *IEEE Transactions on Haptics*, pp. 1–1, 2020.

[22] A. Kaci, A. Torres, F. Giraud, C. Giraud-Audine, M. Amberg, and B. Lemaire-Semail, "Fundamental acoustical finger force calculation for out-of-plane ultrasonic vibration and its correlation with friction reduction," in *2019 IEEE World Haptics Conference (WHC)*. IEEE, 2019, pp. 413–418.

[23] B. Persson, A. Kovalev, and S. Gorb, "Contact mechanics and friction on dry and wet human skin," *Tribology Letters*, vol. 50, no. 1, pp. 17–30, 2013.

[24] B. Mandelbrot, "How long is the coast of britain? statistical self-similarity and fractional dimension," *science*, vol. 156, no. 3775, pp. 636–638, 1967.

[25] A. E. Kovalev, K. Dening, B. N. Persson, and S. N. Gorb, "Surface topography and contact mechanics of dry and wet human skin," *Beilstein journal of nanotechnology*, vol. 5, no. 1, pp. 1341–1348, 2014.

[26] T. André, V. Lévesque, V. Hayward, P. Lefèvre, and J.-L. Thonnard, "Effect of skin hydration on the dynamics of fingertip gripping contact," *Journal of The Royal Society Interface*, vol. 8, no. 64, 2011.

[27] S. Bochereau, B. Dzidek, M. Adams, and V. Hayward, "Characterizing and imaging gross and real finger contacts under dynamic loading," *IEEE transactions on haptics*, vol. 10, no. 4, pp. 456–465, 2017.

[28] B. Dzidek, S. Bochereau, S. A. Johnson, V. Hayward, and M. J. Adams, "Why pens have rubbery grips," *Proceedings of the National Academy of Sciences*, vol. 114, no. 41, pp. 10 864–10 869, 2017.

[29] M. Tada and T. Kanade, "An imaging system of incipient slip for modelling how human perceives slip of a fingertip," in *The 26th Annual International Conference of the IEEE Engineering in Medicine and Biology Society*, vol. 1. IEEE, 2004, pp. 2045–2048.

[30] B. Delhaye, P. Lefevre, and J.-L. Thonnard, "Dynamics of fingertip contact during the onset of tangential slip," *Journal of The Royal Society Interface*, vol. 11, no. 100, p. 20140698, 2014.

[31] B. M. Dzidek, M. J. Adams, J. W. Andrews, Z. Zhang, and S. A. Johnson, "Contact mechanics of the human finger pad under compressive loads," *Journal of The Royal Society Interface*, vol. 14, no. 127, 2017.

[32] M. Wiertlewski and J. E. Colgate, "Power optimization of ultrasonic friction-modulation tactile interfaces," *IEEE transactions on haptics*, vol. 8, no. 1, pp. 43–53, 2014.

[33] J. Monnoyer, E. Diaz, C. Bourdin, and M. Wiertlewski, "Optimal skin impedance promotes perception of ultrasonic switches," in *2017 IEEE World Haptics Conference (WHC)*. IEEE, 2017, pp. 130–135.

[34] T. Soneda and K. Nakano, "Investigation of vibrotactile sensation of human fingerpads by observation of contact zones," *Tribology International*, vol. 43, no. 1-2, pp. 210–217, 2010.

[35] P. H. Warman and A. R. Ennos, "Fingerprints are unlikely to increase the friction of primate fingerpads," *Journal of Experimental Biology*, vol. 212, no. 13, pp. 2016–2022, 2009.

[36] H.-T. Lin, T.-F. Hong, and W.-L. Li, "Grip performance affected by water-induced wrinkling of fingers," *Tribology Letters*, vol. 58, no. 3, p. 38, 2015.

[37] S. M. Pasumarty, S. A. Johnson, S. A. Watson, and M. J. Adams, "Friction of the human finger pad: influence of moisture, occlusion and velocity," *Tribology Letters*, vol. 44, no. 2, p. 117, 2011.

[38] W. B. Messaoud, M. Amberg, B. Lemaire-Semail, F. Giraud, and M.-A. Bueno, "High fidelity closed loop controlled friction in smarttac tactile stimulator," in *2015 17th European Conference on Power Electronics and Applications (EPE'15 ECCE-Europe)*. IEEE, 2015, pp. 1–9.

[39] N. Huloux, J. Monnoyer, M. Boyron, and M. Wiertlewski, "Overcoming the variability of fingertip friction with surface-haptic force-feedback," in *International Conference on Human Haptic Sensing and Touch Enabled Computer Applications*. Springer, 2018, pp. 326–337.